



Published in final edited form as:

Breast J. 2021 April ; 27(4): 314–321. doi:10.1111/tbj.14205.

## Next generation sequencing of breast implant associated anaplastic large cell lymphomas reveals a novel *STAT3-JAK2* fusion among other activating genetic alterations within the *JAK-STAT* pathway

Andrés E. Quesada, M.D.<sup>1</sup>, Yanming Zhang, M.D. Ph.D<sup>1</sup>, Ryan Ptashkin<sup>1</sup>, Caleb Ho, M.D.<sup>1</sup>, Steven Horwitz, M.D.<sup>2</sup>, Ryma Benayed, Ph.D<sup>1</sup>, Ahmet Dogan, M.D.Ph.D<sup>1</sup>, Maria E. Arcila, M.D<sup>1</sup>

<sup>1</sup>Department of Pathology, Memorial Sloan Kettering Cancer Center, New York, NY.

<sup>2</sup>Department of Medicine, Memorial Sloan Kettering Cancer Center, New York, NY.

### Abstract

Breast implant associated anaplastic large cell lymphoma (BIA-ALCL) is a distinct type of ALCL, and a new provisional entity by the 2016 revision of the World Health Organization (WHO) classification of tumors of hematopoietic and lymphoid tissues. In contrast to systemic and primary cutaneous ALCLs, BIA-ALCLs have been genetically characterized by the absence of fusions and frequent activation of the *JAK-STAT3* pathway through mutations in *JAK1* and *STAT3*. In this study, we report the results of the genetic profiling of 9 BIA-ALCL cases supporting the role of the *JAK-STAT* pathway activation in this entity, including the identification of an activating *STAT3-JAK2* fusion similar to those recently reported in T-cell lymphoproliferative disorders of the gastrointestinal tract. To our knowledge, this is the first fusion reported in BIA-ALCL, providing further insight into the overall genetic landscape of this rare entity as well as uncovering potential options for targeted therapy in cases with advanced disease.

### Introduction

Breast implant associated anaplastic large cell lymphoma (BIA-ALCL) has been recently incorporated as a provisional category of ALCL in the 2016 revision of the World Health Organization (WHO) classification of tumors of hematopoietic and lymphoid tissues.<sup>1</sup> This is a rare and distinct entity which arises in the capsule surrounding textured saline or silicone breast implants at a median interval of 9 years and typically presents as a unilateral peri-implant effusion with no grossly identifiable mass lesion. The morphologic and immunophenotypic features are indistinguishable from those of systemic or cutaneous ALK negative ALCL, with the presence of large cells with pleomorphic and anaplastic

**Corresponding author:** Maria E. Arcila, M.D., Memorial Sloan Kettering Cancer Center, Department of Pathology, 1275 York Avenue, New York, NY 10065, arcilam@mskcc.org. Phone: 212-639-7879.

Data Availability Statement

Data available on request from the authors.

Conflict of Interest Disclosure: None.

morphology and characteristic strong / uniform expression of CD30. The prognosis is generally excellent, provided that the disease is confined to the effusion and capsule, as it can be successfully treated with complete capsulectomy alone.<sup>2–5</sup> The presence of an associated mass, invasion through the capsule and lymph node involvement are seen in approximately 20% of patients and are characteristics associated with worse outcome.<sup>6</sup>

While BIA-ALCL appears to have distinct biologic features that set it apart from other ALCL subtypes, the genomic landscape and genetic events specifically responsible for its development remain poorly understood, in part due to the rarity and likely underdiagnosis of the disease. Activating mutations in *STAT3* and *JAK1* have been recently described as common events,<sup>7–10</sup> suggesting that *JAK-STAT3* signaling pathway constitutive activation may be at least partially involved in its oncogenesis.<sup>11,12</sup> To date, however, structural gene rearrangements, including those commonly associated with other ALCLs, such as translocations involving *ALK*, *DUSP22* or *TP63*, have never been reported in BIA-ALCL.<sup>12–15</sup> In this report, we describe the genomic profile of 9 patients with BIA-ALCL using MSK-IMPACT Heme, a 400 gene hybrid capture next generation sequencing assay and the identification of an activating *STAT3-JAK2* fusion not previously described in this entity.

## Materials and Methods

Nine cases with BIA-ALCL diagnosed at our institution were studied. Both DNA and RNA were extracted from sections of formalin-fixed paraffin embedded (FFPE) tumor tissue blocks. To address adequacy issues, between 10–40 sections (5  $\mu$ m thick) were used for extraction. Samples were sequenced using the MSK IMPACT HEME assay, a hybridization capture-based next generation sequencing panel capturing all coding regions of 400 genes<sup>16</sup> and the MSK-PanHeme Fusion assay, an RNA-based gene fusion detection assay which utilizes the ArcherDx Anchored Multiplex polymerase chain reaction (PCR) (AMP™) technology and targets 199 genes. Matched normal control DNA from all 9 patients (4 FFPE non-neoplastic tissue, 3 nail clippings, 2 blood samples) was used for paired tumor: normal analysis to ensure only somatic variant calling. Copy number alterations were assessed using FACETS.<sup>17</sup> To determine T-cell receptor (TCR) beta and TCR gamma gene rearrangement status, conserved regions within the variable (Vb), diversity (Db), and the joining (Jb) regions of TCR beta and gamma were amplified by PCR in the presence of fluorescently-labeled primers (InVivoScribe BIOMED-2), and the amplified products were detected by capillary electrophoresis on an ABI 3730 DNA analyzer (Thermo Fisher Scientific). Fluorescent in-situ hybridization (FISH) was further performed on corresponding FFPE tissue sections using a *JAK2* specific break-apart probe set (Cytocell/Oxford Gene Technology, Tarrytown, NY) following manufacturer's protocol. Immunohistochemical (IHC) staining for pSTAT3 was performed using M9C6 antibody (Cell Signaling Technology, Danvers, MA) at 1:250 dilution on the Leica Bond III staining platform (Leica Biosystems Inc, Buffalo Grove, IL).

## Results

The clinical features of the 9 patients examined in this cohort are provided in Table 1. DNA sequencing was successfully performed on all 9 cases with mean sequencing depth of

461X(range, 184X-678X).Thirty-four somatic mutations were detected across 26 genes in 8 of 9 patients (89%), at a median variant allele frequency (VAF) of 10% (range, 2.3–76.9%). The most commonly mutated gene was *JAK1*, with point mutations involving codon G1097 (D, V or S) identified in 44% (4/9) of the cases. Overall, missense mutations were the most common type of alteration (26/34, 76%) followed by splice site (3/34, 9%), nonsense (3/34, 9%), and frameshift (2/34, 6%) mutations. In all, 78% (7/9) of the cases had a somatic alteration affecting genes in the *JAK/STAT* pathway including *JAK1*, *JAK2*, *STAT3*, *STAT5B* and *SOCS1* and 56% (5/9) had mutations in epigenetic modifiers (Table 2, Figure 1). An in-frame fusion involving exon 24 of *STAT3* and exons 19–25 of *JAK2* (Figure 2) was detected in 1 case. Analysis of copy-number aberrations (CNAs) showed several losses and gains as summarized in Table 2 and Figure 1.

Targeted RNA sequencing (RNASeq) confirmed the fusion transcript and precise breakpoints of the *STAT3-JAK2* rearrangement. No other fusion transcripts were detected by RNAseq on 3 additional cases while the remaining 5 cases could not be successfully sequenced due to low quantity of RNA recovered from the FFPE tissue samples. FISH studies using the *JAK2* break-apart probe confirmed the presence of a *JAK2* rearrangement with a split signal pattern (Figure 3A). No additional *JAK2* rearrangements were detected by FISH, however, 6 of 9 (67%) cases showed extra signals consistent with copy number gains.

TCR gene rearrangement analysis by fragment analysis was successfully performed on all 9 patients and showed clonal rearrangement in 8 of the 9 (89%) cases. One case showed a prominent peak within a polyclonal background.

Immunohistochemical staining for pSTAT3 was performed in 7 of the 9 cases (including the patient with *STAT3-JAK2* fusion). Of the patients tested, 6/7 (86%) showed strong and diffuse expression of pSTAT3.

### Case description

The patient harboring the *STAT3-JAK2* fusion is a 69-year-old woman with history of invasive ductal carcinoma diagnosed in 2003 and treated with bilateral mastectomy and chemotherapy. Initial reconstructive surgery with placement of breast silicone implants was performed in 2004, followed by implant replacement in 2010. In 2018, she developed left breast swelling and a pericapsular effusion. Cytologic assessment of aspirated fluid revealed atypical cells suspicious for lymphoma. Concurrent flow cytometric analysis confirmed the presence of abnormal cells with aberrant immunophenotype (18.9% of the total white cells), including bright expression of CD30, CD45, and CD56, as well as increased forward and side scatter suggestive of larger size but without expression of CD2, CD3, CD4, CD5, CD7, CD8, CD10, CD19, CD20, CD22, CD23, CD38, CD200, CD279, or FMC7. Subsequent complete capsulectomy confirmed involvement by BIA-ALCL (Figure 3B).<sup>4,5</sup> There was no mass formation, extracapsular extension or lymphadenopathy. Immunohistochemical stains (Figure 3B) showed strong positivity for CD30 and lack of ALK1 or pan-cytokeratin expression; pSTAT3 showed strong expression in the neoplastic cells. The patient is currently doing well on expectant monitoring with no adjuvant therapy given.

## Discussion

In the present study, we report the sequencing results of 9 BIA-ALCL cases including, to our knowledge, the first fusion identified in this entity. To date, the overall understanding of the genetic landscape of BIA-ALCL remains limited due to the relatively small number of cases studied. Based on review of literature, only 57 total cases have been previously studied using NGS, of which 24 underwent whole exome sequencing<sup>7-10,18,19</sup> while others were studied using narrow targeted panels.

In keeping with prior reports, our study supports that the *JAK-STAT* pathway is frequently dysregulated in BIA-ALCL. Both activating and putative loss-of function mutations were identified within this pathway in 78% of cases. *JAK2* copy number gains were identified by FISH analysis in the remaining cases which could potentially elicit or enhance aberrant activation of the *JAK-STAT3* pathway.<sup>20</sup> Immunohistochemistry for expression of pSTAT3 was also positive in all cases tested except for one. In contrast to prior studies, mutations in the JH1 kinase domain of *JAK1*, rather than STAT3, were the most common variants in our cohort (44% of cases). Alterations involved codon G1097 exclusively (G1097D, G1097S and G1097V), all of which are well recognized gain-of-function mutations which trigger aberrant phosphorylation of *STAT3* downstream in hematologic malignancies. Other alterations involving this pathway included mutations in *STAT3*, *STAT5* and *SOCS1*. The *STAT3* mutation, S614R, has been previously described as the most common activating mutation in BIA-ALCL in all previous studies, while the *STAT5B* mutation is a variant not previously reported. A *SOCS1* truncating mutation with putative loss-of-function effect was also detected, predicting deregulation through to loss of inhibition on *JAK-STAT* signaling. Similar mutations in this gene have been identified in various types of lymphomas, including BIA-ALCL.<sup>21-24</sup>

Of particular interest, the *STAT-JAK2* fusion detected in this study was recently reported as a recurrent genetic alteration in indolent T-cell lymphoproliferative disorder of the gastrointestinal tract (GI TLPDs).<sup>25</sup> To date, only 4 cases have been reported in the literature, exclusively associated with GI TLPDs. The finding of a similar fusion in a similarly indolent process may support the potential role of these rearrangements in a distinct subset of less aggressive lymphoproliferative disorders. Similar to the previously reported fusions, the *STAT3-JAK2* rearrangement in BIA-ALCL retains the entire catalytic domain (JH1) of *JAK2* and shares the same *STAT3* RNA breakpoint. Recent functional studies performed by Hu et al, confirm this fusion to be oncogenic both in vitro and in-vivo using various models.<sup>26</sup> Coincidentally, to specifically assess function in human T-cell lymphoma model, this group evaluated the effect of the fusion on the growth of TLBR-3 cells derived from a BIA-ALCL, which are dependent on IL2. Fusion expression rescued the cells from IL2 withdrawal causing marked independent growth in vitro as well as large subcutaneous tumor formation in-vivo on NSG mice. Studies also demonstrated that fusion expression activates STAT5 and constitutively enhances transcriptional activity within the *JAK-STAT* pathway. More importantly, preliminary work by the same group using various JAK inhibitors in-vitro and in an animal model, characterize this fusion as a potential targetable event with differential impact on the activity of the fusion protein.<sup>26</sup>

*JAK2* fusions or rearrangements involving other partners have been identified in a variety of myeloid and precursor lymphoid neoplasms<sup>27,28</sup> but are rare in mature T-cell lymphomas.<sup>29–32</sup> In a previous study by Ehrentraut et al., for example, the authors used a FISH break apart probe to assess for *JAK2* rearrangements in 200 patients with various T-cell lymphomas, including 53 patients with ALCL and ALCL cell lines, finding no evidence of *JAK2* fusions in any of the samples studied.<sup>31</sup> Although our combined assessment for fusions using DNA and RNA in this study was partially limited by the quality and quantity of RNA that could be effectively isolated from some of the samples, targeted FISH analysis did not identify any other *JAK2* rearrangement outside of our index case.

In addition to alterations involving the *JAK-STAT* pathway, somatic events involving epigenetic modifiers were the second most common alterations identified. Mutations or gene losses involving *TET2*, *TET3*, *ARID4B*, *KDM5C*, *KDM6A*, *KMT2C/D*, and *SMARCB1* were detected in 56% of cases. Alterations in epigenetic modifiers are common in T-cell lymphomas and have also been recently reported as common events in the largest series of BIA-ALCL studied by NGS.<sup>19</sup>

Taken together, while our current understanding of the genetics of BIA-ALCL still remains limited, thus far, a unifying mechanism of lymphomagenesis in this rare entity seems to be the activation of the *JAK-STAT* pathway which also offers possibilities for targeted treatment in patients with advanced disease. A more recent finding is the accumulation of alterations in epigenetic modifiers which are also common in other T-cell lymphomas. These findings also have important diagnostic and therapeutic implications. Diagnostically, the presence of mutations, while not necessarily diagnostic of the entity itself, could greatly facilitate the diagnosis of BIA-ALCL in conjunction with the morphologic and immunophenotypic findings and could also provide a molecular marker for staging and monitoring.

Although the majority of patients diagnosed with BIA-ALCL can be cured with complete capsulectomy alone, those that present with a mass lesion or disease beyond the capsule are considered high risk for recurrence and progression.<sup>6</sup> Within our small cohort, for instance, patients 4 and 8 presented with advanced disease, requiring systemic therapy and radiotherapy and one ultimately required stem cell transplant as outlined in table 1. Patients with advanced disease often constitute a therapeutic challenge for current treatment modalities, underscoring the need to explore alternate therapeutic options. At present, significant pre-clinical and early clinical data support the potential efficacy of therapies targeting the *JAK-STAT* pathway and epigenetic regulators, with several clinical trials currently underway, underscoring the importance of comprehensively evaluating patients for potential therapeutic targets.

An important and critical consideration for future studies, is the adequate preservation of material for broad molecular testing. Two recent publications by Jaffe, et al and Lyapichev, et al outline key strategies in processing of these roma fluid/effusion surrounding the implant and the handling of capsulectomy specimens following removal of implant(s).<sup>33,34</sup> Of note, based on our own experience, we find that while these guidelines effectively address the basic needs for morphologic and immunophenotypic assessment in clinical

practice, comprehensive molecular testing remains a challenge. Due to the nature of this disease, involvement of the capsule is often very focal, making it difficult to obtain sufficient tumor from FFPE capsule tissue. Alternatively, the effusion fluid may contain many more tumor cells than the capsule itself and could provide more material for downstream studies but the recommendations to prioritize the creation of a cell block over fresh material for flow cytometry and other studies, limit the amount and quality of material that can be recovered for molecular assays, particularly for RNA studies. In our small series, despite extensive efforts to maximize tumor and nucleic acid yield by using up to 40 sections of FFPE tissue, most samples could not be tested by RNA seq due to low quantity and quality of RNA. In light of the scant nature of the material, protocols designed for maximal preservation of fresh pericapsular fluid for molecular studies would be highly valuable to obtain high quality sequencing data. The concentration of the cellular content by centrifugation from larger volumes of pericapsular fluid would also greatly facilitate future studies.

## Acknowledgments

The data that support the findings of this study are available from the corresponding author upon reasonable request.

## References

1. Feldman AL, Harris NL, Stein H, et al. Breast implant-associated anaplastic large cell lymphoma. In: Swerdlow SH, Campo E, Harris NL, Jaffe ES, Pileri SA, Stein H, Thiele J (Eds). WHO Classification of Tumours of Haematopoietic and Lymphoid Tissues (Revised 4th Edition). IARC: Lyon; 2017.
2. Miranda RN, Aladily TN, Prince HM, et al. Breast implant-associated anaplastic large-cell lymphoma: long-term follow-up of 60 patients. *J Clin Oncol*. 2014;32(2):114–120. [PubMed: 24323027]
3. Clemens MW, Medeiros LJ, Butler CE, et al. Complete Surgical Excision Is Essential for the Management of Patients With Breast Implant-Associated Anaplastic Large-Cell Lymphoma. *J Clin Oncol*. 2016;34(2):160–168. [PubMed: 26628470]
4. Clemens MW, Jacobsen ED, Horwitz SM. 2019 NCCN Consensus Guidelines on the Diagnosis and Treatment of Breast Implant-Associated Anaplastic Large Cell Lymphoma (BIA-ALCL). *Aesthet Surg J*. 2019;39(Supplement\_1):S3–S13. [PubMed: 30715173]
5. Quesada AE, Medeiros LJ, Clemens MW, Ferrufino-Schmidt MC, Pina-Oviedo S, Miranda RN. Breast implant-associated anaplastic large cell lymphoma: a review. *Mod Pathol*. 2019;32(2):166–188. [PubMed: 30206414]
6. Ferrufino-Schmidt MC, Medeiros LJ, Liu H, et al. Clinicopathologic Features and Prognostic Impact of Lymph Node Involvement in Patients With Breast Implant-associated Anaplastic Large Cell Lymphoma. *Am J Surg Pathol*. 2018;42(3):293–305. [PubMed: 29194092]
7. Blombery P, Thompson ER, Jones K, et al. Whole exome sequencing reveals activating JAK1 and STAT3 mutations in breast implant-associated anaplastic large cell lymphoma anaplastic large cell lymphoma. *Haematologica*. 2016;101(9):e387–390. [PubMed: 27198716]
8. Di Napoli A, Jain P, Duranti E, et al. Targeted next generation sequencing of breast implant-associated anaplastic large cell lymphoma reveals mutations in JAK/STAT signalling pathway genes, TP53 and DNMT3A. *Br J Haematol*. 2018;180(5):741–744. [PubMed: 27859003]
9. Letourneau A, Maerevoet M, Milowich D, et al. Dual JAK1 and STAT3 mutations in a breast implant-associated anaplastic large cell lymphoma. *Virchows Arch*. 2018;473(4):505–511. [PubMed: 29637270]
10. Oishi N, Brody GS, Ketterling RP, et al. Genetic subtyping of breast implant-associated anaplastic large cell lymphoma. *Blood*. 2018;132(5):544–547. [PubMed: 29921615]



11. Crescenzo R, Abate F, Lasorsa E, et al. Convergent mutations and kinase fusions lead to oncogenic STAT3 activation in anaplastic large cell lymphoma. *Cancer Cell*. 2015;27(4):516–532. [PubMed: 25873174]
12. Oishi N, Miranda RN, Feldman AL. Genetics of Breast Implant-Associated Anaplastic Large Cell Lymphoma (BIA-ALCL). *Aesthet Surg J*. 2019;39(Supplement\_1):S14–S20. [PubMed: 30715169]
13. Parrilla Castellar ER, Jaffe ES, Said JW, et al. ALK-negative anaplastic large cell lymphoma is a genetically heterogeneous disease with widely disparate clinical outcomes. *Blood*. 2014;124(9):1473–1480. [PubMed: 24894770]
14. Feldman AL, Dogan A, Smith DI, et al. Discovery of recurrent t(6;7)(p25.3;q32.3) translocations in ALK-negative anaplastic large cell lymphomas by massively parallel genomic sequencing. *Blood*. 117(3):915–919. [PubMed: 21030553]
15. Vasmatzis G, Johnson SH, Knudson RA, et al. Genome-wide analysis reveals recurrent structural abnormalities of TP63 and other p53-related genes in peripheral T-cell lymphomas. *Blood*. 120(11):2280–2289.
16. Ptashkin RN, Benayed R, Ziegler J, et al. MSK-IMPACT Heme: Validation and clinical experience of a comprehensive molecular profiling platform for hematologic malignancies [abstract]. In: Proceedings of the American Association for Cancer Research Annual Meeting 2019; 2019 Mar 29-Apr 3; Atlanta, GA. Philadelphia (PA): AACR; Cancer Res. 2019;79(13 Suppl):Abstract nr 3409.
17. Shen R, Seshan VE. FACETS: allele-specific copy number and clonal heterogeneity analysis tool for high-throughput DNA sequencing. *Nucleic Acids Res*. 2016;44(16):e131. [PubMed: 27270079]
18. Laurent C, Delas A, Gaulard P, et al. Breast Implant Associated Anaplastic Large cell Lymphoma: two distinct clinicopathological variants with different outcomes. *Ann Oncol*. 2015.
19. Laurent C, Nicolae A, Laurent C, et al. Gene alterations in epigenetic modifiers and JAK-STAT signaling are frequent in breast implant-associated ALCL. *Blood*. 2020;135(5):360–370. [PubMed: 31774495]
20. Quintas-Cardama A, Verstovsek S. Molecular pathways: Jak/STAT pathway: mutations, inhibitors, and resistance. *Clin Cancer Res*. 2013;19(8):1933–1940. [PubMed: 23406773]
21. Mottok A, Renne C, Seifert M, et al. Inactivating SOCS1 mutations are caused by aberrant somatic hypermutation and restricted to a subset of B-cell lymphoma entities. *Blood*. 2009;114(20):4503–4506. [PubMed: 19734449]
22. Weniger MA, Melzner I, Menz CK, et al. Mutations of the tumor suppressor gene SOCS-1 in classical Hodgkin lymphoma are frequent and associated with nuclear phospho-STAT5 accumulation. *Oncogene*. 2006;25(18):2679–2684. [PubMed: 16532038]
23. Juskevicius D, Lorber T, Gsponer J, et al. Distinct genetic evolution patterns of relapsing diffuse large B-cell lymphoma revealed by genome-wide copy number aberration and targeted sequencing analysis. *Leukemia*. 2016;30(12):2385–2395. [PubMed: 27198204]
24. Ehrentraut S, Schneider B, Nagel S, et al. Th17 cytokine differentiation and loss of plasticity after SOCS1 inactivation in a cutaneous T-cell lymphoma. *Oncotarget*. 2016;7(23):34201–34216.
25. Sharma A, Oishi N, Boddicker RL, et al. Recurrent STAT3-JAK2 fusions in indolent T-cell lymphoproliferative disorder of the gastrointestinal tract. *Blood*. 2018;131(20):2262–2266. [PubMed: 29592893]
26. Hu G, Phillips JL, Dasari S, et al. Targetability of STAT3-JAK2 fusions: implications for T-cell lymphoproliferative disorders of the gastrointestinal tract. *Leukemia*. 2020;34(5):1467–1471. [PubMed: 31836854]
27. Lacronique V, Boureux A, Valle VD, et al. A TEL-JAK2 fusion protein with constitutive kinase activity in human leukemia. *Science*. 1997;278(5341):1309–1312. [PubMed: 9360930]
28. Smith CA, Fan G. The saga of JAK2 mutations and translocations in hematologic disorders: pathogenesis, diagnostic and therapeutic prospects, and revised World Health Organization diagnostic criteria for myeloproliferative neoplasms. *Hum Pathol*. 2008;39(6):795–810. [PubMed: 18538168]
29. Adelaide J, Perot C, Gelsi-Boyer V, et al. A t(8;9) translocation with PCM1-JAK2 fusion in a patient with T-cell lymphoma. *Leukemia*. 2006;20(3):536–537. [PubMed: 16424865]

30. Davis TH, Morton CC, Miller-Cassman R, Balk SP, Kadin ME. Hodgkin's disease, lymphomatoid papulosis, and cutaneous T-cell lymphoma derived from a common T-cell clone. *N Engl J Med*. 1992;326(17):1115–1122. [PubMed: 1532439]
31. Ehrentraut S, Nagel S, Scherr ME, et al.t(8;9)(p22;p24)/PCM1-JAK2 activates SOCS2 and SOCS3 via STAT5. *PLoS One*. 2013;8(1):e53767. [PubMed: 23372669]
32. Panagopoulos I, Gorunova L, Spetalen S, et al.Fusion of the genes ataxin 2 like, ATXN2L, and Janus kinase 2, JAK2, in cutaneous CD4 positive T-cell lymphoma. *Oncotarget*. 2017;8(61):103775–103784. [PubMed: 29262599]
33. Jaffe ES, Ashar BS, Clemens MW, et al.Best Practices Guideline for the Pathologic Diagnosis of Breast Implant-Associated Anaplastic Large-Cell Lymphoma. *J Clin Oncol*. 2020;38(10):1102–1111. [PubMed: 32045544]
34. Lyapichev KA, Pina-Oviedo S, Medeiros LJ, et al.A proposal for pathologic processing of breast implant capsules in patients with suspected breast implant anaplastic large cell lymphoma. *Mod Pathol*. 2020;33(3):367–379. [PubMed: 31383966]





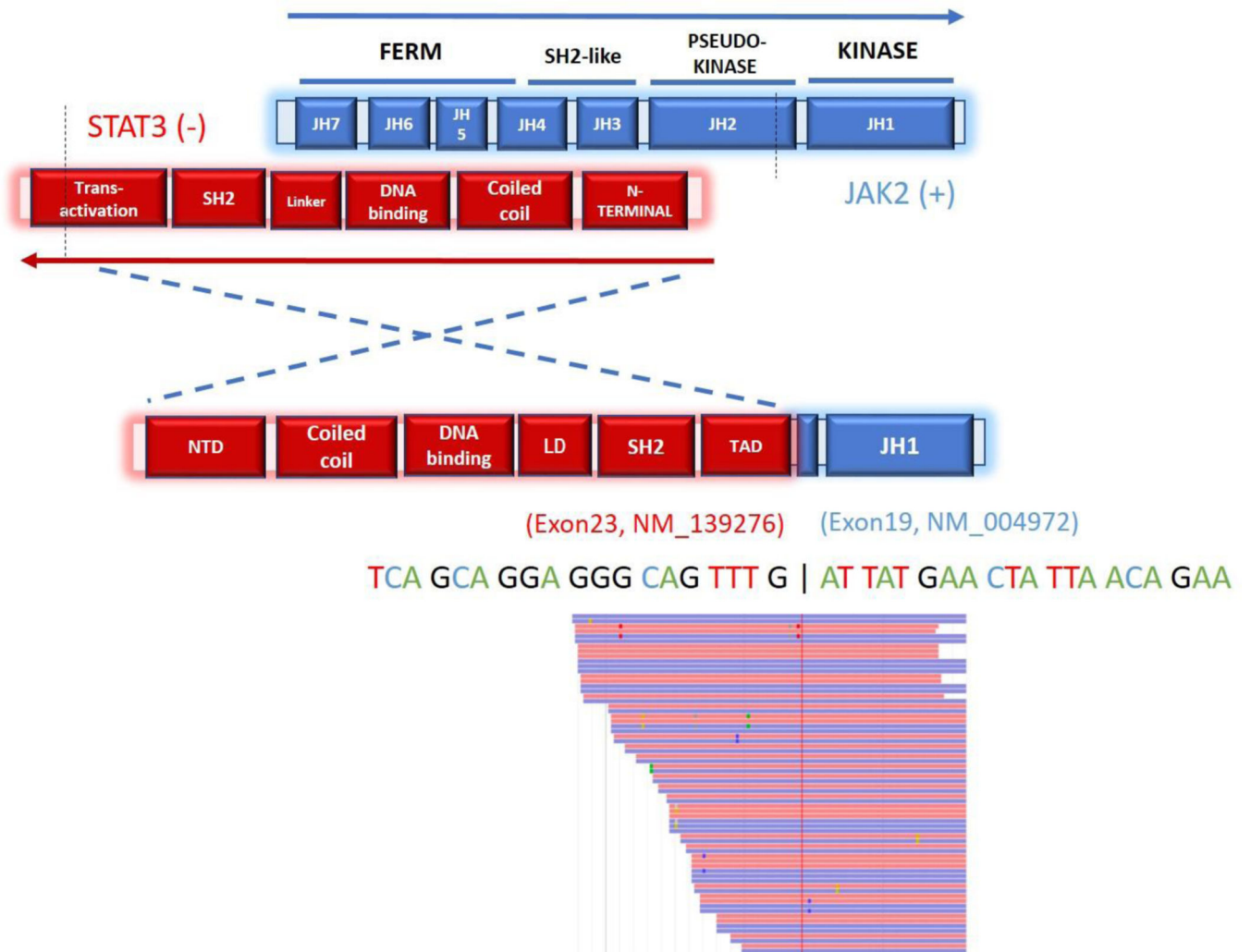


**Figure 2.** Schematic illustration of the protein structure and transcript sequence of the *STAT3-JAK2* in-frame fusion product. Exons 1–23 of *STAT3* are fused to exons 19–25 of *JAK2* which include the kinase domain. Red and blue rectangles represent bi-directional RNA sequencing reads supporting the fusion breakpoint.

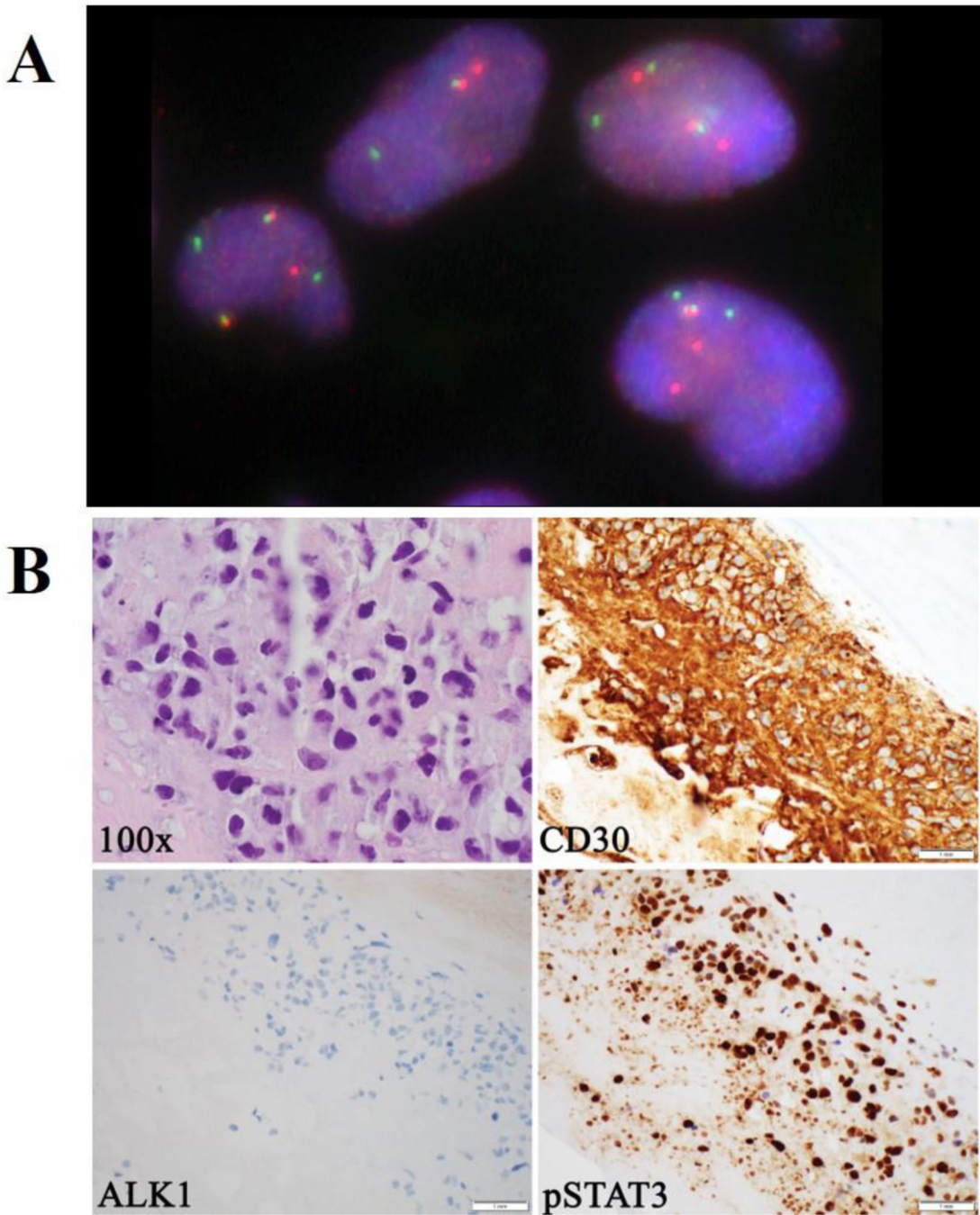


**Figure 3.**

A, Fluorescence in situ hybridization performed on FFPE using a *JAK2* specific break-apart probe set showing a split signal pattern, indicative of a *JAK2* rearrangement. B, Large anaplastic cells with irregular and multilobated nuclei with occasional “hallmark” cells (H&E, 1000x, oil immersion); the anaplastic cells strongly and uniformly express CD30 (400x); the cells lack expression of ALK1 (400x); the anaplastic cells show strong expression of pSTAT3 (400x).

**Table 1.** Clinicopathologic features of 9 patients with breast implant associated anaplastic large cell lymphoma.

Patient	Age	Reason for Implant	Type of Implant	Number of Years after Implant	Presentation	Stage	Treatment	pSTAT IHC
1	68	IDC	Textured	8	Left breast swelling	T2	Bilateral complete capsulectomies	Positive
2	77	IDC	Textured	12	Right breast mass	T4, stage IIA	Excision and complete capsulectomy	Positive
3	61	IDC and ILC	Textured	8	Right breast swelling, effusion	T1*	Bilateral complete capsulectomies	N/A
4	58	DCIS	Textured	6	Firmness above her left breast implant and change in shape of implant	T4N2M0	Capsulectomy and BV-CHP x 6 cycles + consolidative radiotherapy (3060 cGY in 17 fractions)	Positive
5	65	IDC	Textured	10	Right breast effusion	T1*	Complete capsulectomy	Positive
6	35	Cosmetic	Textured	8	Right breast swelling, effusion	T1	Bilateral complete capsulectomies	N/A
7	51	IDC	Textured	6	Left breast swelling, effusion	T1, stage IA	Bilateral complete capsulectomies	Positive
8	66	IDC	Textured	11	Cutaneous lesion	T4	XRT (15 fractions, total 3000cGY)-, 6 cycles BV-CHOP, SCT	Negative
9	50	ILC	Textured	6	Left breast swelling, fevers, night sweats	T3, stage 1C	Bilateral complete capsulectomies	Positive

IDC, invasive ductal carcinoma; ILC, invasive lobular carcinoma; DCIS, ductal carcinoma in situ; SCT, stem cell transplant; IHC, Immunohistochemistry;

\* Lymphoma confined to fluid only

**Table 2.**

Alterations detected by 400 gene hybrid capture next generation sequencing panel in 9 patients with breast implant associated anaplastic large cell lymphoma.

Patient	Gene Altered	Reference Sequence	Protein Change	cDNA Change	Location	Type of Alteration	VAF (%)	JAK2 FISH Results	FACETS Results
1	<i>TP53</i> <i>MGAM</i> <i>PAK7</i> <i>SMARCB1</i>	NM_000546	p.A307P	c.919G>C	exon 8	Missense	6.9	<i>JAK2</i> translocation positive; 70% large cells, complex patterns	No calls
		NM_004668	p.X1449_splice	c.4345+1G>A	exon 36	Splice	9.9		
	<i>STAT3-JAK2</i>	NM_177990	p.P358R	c.1073C>G	exon 5	Missense	3.9		
		NM_003073	p.Q368*	c.1102C>T	exon 8	Nonsense	8.4		
2	<i>ATM</i> <i>JAK1</i> <i>JARID2</i> <i>TET3</i> <i>TET3</i>	NM_139276	t(17;9)(q21.1)			Fusion			
		NM_004972							
3	<i>TET2</i> <i>JAK1</i> <i>STAT5B</i>	NM_000051	p.M900I	c.2700G>C	exon 18	Missense	5.1	Gain of extra copies; 3-5 signals, 50-60%	No calls
		NM_002227	p.G1097S	c.3289G>A	exon 24	Missense	27		
	<i>TET2</i> <i>JAK1</i> <i>STAT5B</i>	NM_004973	p.V1019L	c.3055G>C	exon 14	Missense	8.6		
		NM_144993	p.V595L	c.1783G>T	exon 1	Missense	15.8		
4	<i>BCR</i> <i>JAK1</i> <i>SMARCB1</i>	NM_144993	p.V787I	c.2359G>A	exon 4	Missense	17.1		
		NM_001127208	p.Q960*	c.2878C>T	exon 3	Nonsense	2.4		
	<i>BCR</i> <i>JAK1</i> <i>SMARCB1</i>	NM_002227	p.G1097D	c.3290G>A	exon 24	Missense	10.1		
		NM_012448	p.I174S	c.521T>G	exon 5	Missense	5.6		
5	<i>ARID4B</i> <i>BRP1</i> <i>DDR2</i> <i>DDX3X</i> <i>JAK1</i>	NM_004327	p.R162C	c.484C>T	exon 1	Missense	34.4	Normal	Gain: 1p32-36, 2p (including <i>ALK</i> , <i>REL</i> ), 2q11-35, 6p, 17q11-21, Xq25, Xq26.1, Xq26.2 (including <i>STAT2</i> , <i>BCORL1</i> , and <i>PHF6</i> ) CNLOH: SP140 Loss: on 1p ( <i>JAK1</i> , <i>BCL10</i> ), 12q13 (including <i>ARID2</i> , <i>HDAC7</i> and <i>KMT2D/MLL2</i> ), 16q23 (including <i>PLCG3</i> , <i>IRF8</i> and <i>FANCA</i> ), 20p and 20q12-13, Xq12 (AR)
		NM_002227	p.G1097D	c.3290G>A	exon 24	Missense	41.4		
	<i>ARID4B</i> <i>BRP1</i> <i>DDR2</i> <i>DDX3X</i> <i>JAK1</i>	NM_003073	p.D101N	c.301G>A	exon 3	Missense	25.5		
		NM_016374	p.P134A	c.400C>G	exon 7	Missense	11.6		
	<i>ARID4B</i> <i>BRP1</i> <i>DDR2</i> <i>DDX3X</i> <i>JAK1</i>	NM_032043	p.G763A	c.2288G>C	exon 16	Missense	33	Gain of extra copies; 3-4 signals, 30-40%	Gain: 8q, 17q
		NM_006182	p.X189_splice	c.566-2A>G	exon 7	Splice	9.7		
	<i>ARID4B</i> <i>BRP1</i> <i>DDR2</i> <i>DDX3X</i> <i>JAK1</i>	NM_001356	p.G533E	c.1598G>A	exon 14	Missense	13.4		
		NM_002227	p.G1097V	c.3290G>T	exon 24	Missense	36		
	<i>ARID4B</i> <i>BRP1</i> <i>DDR2</i> <i>DDX3X</i> <i>JAK1</i>	NM_198159	p.E303V	c.908A>T	exon 7	Missense	7		
		NM_001042424	p.X961_splice	c.2882-28_2895del	exon 16	Splice	11.3		

Patient	Gene Altered	Reference Sequence	Protein Change	cDNA Change	Location	Type of Alteration	VAF (%)	JAK2 FISH Results	FACETS Results
6	<i>MTF</i> <i>WHSC1</i>	N/A	N/A	N/A	N/A	N/A	N/A	Gain of extra copies; 3-5 signals, 60-80%	No calls
7	<i>JARID2</i> <i>SOC31</i>	NM_004973 NM_003745	p.A700V p.S32Ffs*44	c.2099C>T c.95_142delins TCCTTCCTCCTCCTCGCCCG	exon 8 exon 2	Missense Frameshift, deletion	37.9 76.9	Gain of extra copies; 3 signals, 10-20%	Gain: 2p, 2q11-35, 17q11-21, ASXL1 (20q11.21) CNLOH: HDAC4, chr22q Loss: 1p22.3-p12, 20p, 20q12-13
8	<i>AXIN1</i> <i>GNA5</i> <i>KDM6A</i> <i>RARA</i>	NM_003502 NM_000516 NM_021140 NM_000964	p.Q476* p.R201C p.V1113Sfs*8 p.R272W	c.1426C>T c.601C>T c.3334_3335dupGT c.814C>T	exon 6 exon 8 exon 23 exon 7	Nonsense Missense Frameshift, insertion Missense	2.3 2.4 14.2 41.1	Gain of extra copies; 3-4 signals, 40-50%	No calls
9	<i>PIK3CA</i> <i>STAT3</i> <i>KMT2B</i> <i>KMT2C</i> <i>KMT2C</i> <i>NCOR2</i>	NM_006218 NM_139276 NM_014727 NM_170606 NM_170606 NM_006312	p.H1047R p.S614R S1739F L596V S593L S1518L	c.3140A>G c.1842C>G c.5216C>T c.1786C>G c.1778C>T c.4553C>T	exon 21 exon 20 exon 25 exon 13 exon 13 exon 34	Missense Missense Missense Missense Missense Missense	3.2 7.7 14.3 5.9 6.1 5.2	Gain of extra copies; 3-4 signals, 50-60%	No calls

VAF, variant allele frequency; Chr, chromosome; CNLOH, copy neutral loss of heterozygosity; FISH, fluorescence in situ hybridization.